UDK 620.186:621.78
Original scientific article/Izvirni znanstveni članek

ISSN 1580-2949
MTAEC9, 48(5)679(2014)

MICROSTRUCTURAL COMPARISON OF THE THERMOMECHANICALLY TREATED AND COLD DEFORMED Nb-MICROALLOYED TRIP STEEL

PRIMERJAVA MIKROSTRUKTUR TERMOMEHANSKO OBDELANEGA IN HLADNO DEFORMIRANEGA, Z Nb-MIKROLEGIRANEGA TRIP-JEKLA

Adam Grajcar[1], Krzysztof Radwański[2]

[1]Silesian University of Technology, Institute of Engineering Materials and Biomaterials, 18a Konarskiego Street, 44-100 Gliwice, Poland
[2]Institute for Ferrous Metallurgy, 12-14 K. Miarki Street, 44-100 Gliwice, Poland
adam.grajcar@polsl.pl

Prejem rokopisa – received: 2013-09-30; sprejem za objavo – accepted for publication: 2013-11-04

The work deals with a microstructural comparison of the thermomechanically processed and subsequently cold deformed Nb-microalloyed Si-Al-type multiphase steel, showing a TRIP effect. The newly developed steel was subjected to the thermomechanical rolling and controlled cooling under the conditions allowing us to obtain a fine-grained ferritic-bainitic microstructure with a large fraction of the retained austenite. Subsequently, the thermomechanically rolled sheet samples were subjected to a 10 % elongation in uniaxial tension. The comparison of the multiphase microstructures and, especially, the identification of the strain-induced martensite were carried out using light microscopy, electron transmission microscopy and electron scanning microscopy equipped with EBSD (electron backscatter diffraction). Morphological details influencing the mechanical stability of the retained austenite were indicated.

Keywords: thermomechanical treatment, TRIP effect, multiphase steel, retained austenite, strain-induced martensite, EBSD technique

Delo obravnava primerjavo mikrostruktur termomehansko obdelanega in nato hladno deformiranega, z Nb-mikrolegiranega večfaznega jekla Al-Si, ki izkazuje vedenje TRIP. Novo razvito jeklo je bilo termomehansko valjano in kontrolirano ohlajeno v razmerah, ki omogočajo doseganje drobnozrnate feritno-bainitne mikrostrukture z velikim deležem zaostalega avstenita. Termomehansko izvaljani vzorci pločevine so bili nato izpostavljeni 10-odstotnemu raztezku pri enoosni natezni obremenitvi. Primerjava multifaznih mikrostruktur in posebno določanje napetostno induciranega martenzita je bila izvršena s svetlobno mikroskopijo, elektronsko presevno mikroskopijo in elektronsko vrstično mikroskopijo, opremljeno z EBSD (Electron Backscatter Diffraction). Prikazane so morfološke podrobnosti, ki vplivajo na mehansko stabilnost zaostalega avstenita.

Ključne besede: termomehanska obdelava, učinek TRIP, večfazno jeklo, zaostali avstenit, napetostno inducirani martenzit, EBSD-tehnika

1 INTRODUCTION

The mechanical properties and technological formability of advanced high-strength steels (AHSS) for the automotive industry depend on the relative proportions and mechanical properties of individual microstructural constituents. Ferrite forms a matrix of AHSS whereas the strengthening phases consist of martensite and/or bainite. A very attractive combination of high strength and ductility can be obtained in dual-phase (DP) steels consisting of a ferrite matrix and uniformly distributed martensitic or martensitic-bainitic islands.[1–4] A further growth of the strength-ductility balance can be obtained for the steels with a ferritic matrix containing bainitic-austenitic islands, where the final mechanical properties are formed during cold working under the conditions of the strain-induced martensitic transformation of the metastable retained austenite.[5–8] Multiphase steel sheets are produced with the continuous annealing of cold-rolled sheets[3,7] or they are thermomechanically hot rolled and controlled cooled.[8,9] A further increase in the strength properties of multiphase steels requires modified chemical-composition concepts. Recently, Nb, Ti and V microalloying has been used to enhance the strength of multiphase steels[8–10], well known for its beneficial effect in HSLA steels.[11–15]

Thermomechanically processed multiphase steels are characterized by a high-grain refinement. Therefore, the qualitative and quantitative identifications of individual structural constituents are especially important. A determination of the γ-phase volume fraction is achieved using a computer-image analysis after the colour etching, X-ray or neutron diffraction and magnetic methods.[5,6,8,16] Recently, the EBSD technique of a scanning electron microscope (SEM) has had an essential significance in determining the fractions and morphological features of various microstructural constituents.[17–19] Microstructural details of cold-rolled multiphase steels have been characterized to a sufficient extent.[7,17–19] However, there are very few reports concerning morphological details of thermomechanically rolled TRIP steels.[9] Hence, the present study addresses the microstructure evolution of a hot-rolled Nb-microalloyed Si-Al multiphase steel.

2 EXPERIMENTAL PROCEDURE

The chemical composition of the newly developed steel was designed with the focus on maximizing the retained-austenite fraction and obtaining the carbide-free bainite. The steel contains: 0.24 % C, 1.55 % Mn, 0.87 % Si, 0.40 % Al, 0.034 % Nb, 0.023 % Ti, 0.004 % S and 0.010 % P. Nb and Ti were used to increase the strength and to achieve the grain refinement during hot rolling. The ingot was produced with vacuum induction melting and then it was hot forged to a thickness of 22 mm. Subsequently, the flat samples were roughly rolled to a thickness of 4.5 mm within the temperature range between 1200 °C and 900 °C. The thermomechanical rolling was conducted in 3 passes between 1100 °C and 850 °C to the final sheet thickness of about 2 mm. After the final deformation at 850 °C the specimens were air cooled to 700 °C and then slowly to the temperature of 650 °C for 50 s using furnace cooling. The next step included immerse cooling of the sheets at a rate of about 50 °C/s, using a water-polymer medium, to the isothermal holding temperature (450 °C) at the bainitic transformation range. The specimens were held at 450 °C for 600 s and finally cooled at a rate of about 0.5 °C/s to room temperature. Then, standard-sized, A50 tensile-test samples with a gauge length of 50 mm and a width of 12.5 mm were cut parallel to the rolling direction of the sheets and deformed to 10 % of the plastic strain at a strain rate of 5×10^{-3} s^{-1}. Metallographic specimens were taken at different points along the rolling direction for both thermomechanically processed samples and those subjected to cold deformation.

For the purpose of a detailed analysis of all the microstructural constituents and, especially, to identify the strain-induced martensitic transformation, light microscopy (LM), scanning electron microscopy (SEM) and transmission electron microscopy (TEM) were used. Additionally, orientation imaging microscopy (OIM) using SEM was applied. Etching in a 10 % aqueous solution of sodium metabisulfite was used. Metallographic observations at the magnification of 1000-times were carried out with a Leica MEF 4A light microscope. Morphological details of microstructural constituents of the steel were revealed with SUPRA 25 SEM using back-scattered electrons (BSE). Observations were performed on nital-etched samples at the accelerating voltage of 20 kV. The EBSD technique was performed using Inspect F SEM equipped with Shottky field emission. After the classical grinding and polishing, the specimens were polished with Al_2O_3 with a granularity of 0.1 μm. The final stage of the sample preparation was the ion polishing using the GATAN 682 PECS system. A fraction of the retained austenite in both the initial state and after cold deformation, assessed with EBSD (the average value of five measurements) was determined at a magnification lower than 3000-times to obtain reliable quantitative results.

The thin-foil investigations were carried out using a JEOL JEM 3010 at the accelerating voltage of 200 kV. Mechanically grinded disk specimens were polished at the voltage of 17 V and current density of 0.2 A/cm^2. The mixture of 490 mL H_3PO_4 + 7 mL H_2SO_4 + 50 g CrO_3 was used as the electrolyte.

3 RESULTS AND DISCUSSION

Applying the thermomechanical rolling and controlled cooling results in a fine-grained ferritic matrix with a volume fraction of about 60 % containing uniformly distributed bainitic-austenitic and austenitic islands (**Figure 1a**). The amount of the retained austenite determined by EBSD is about 13.8 %. The carbon content (C_γ) of the γ phase determined earlier[8] using the

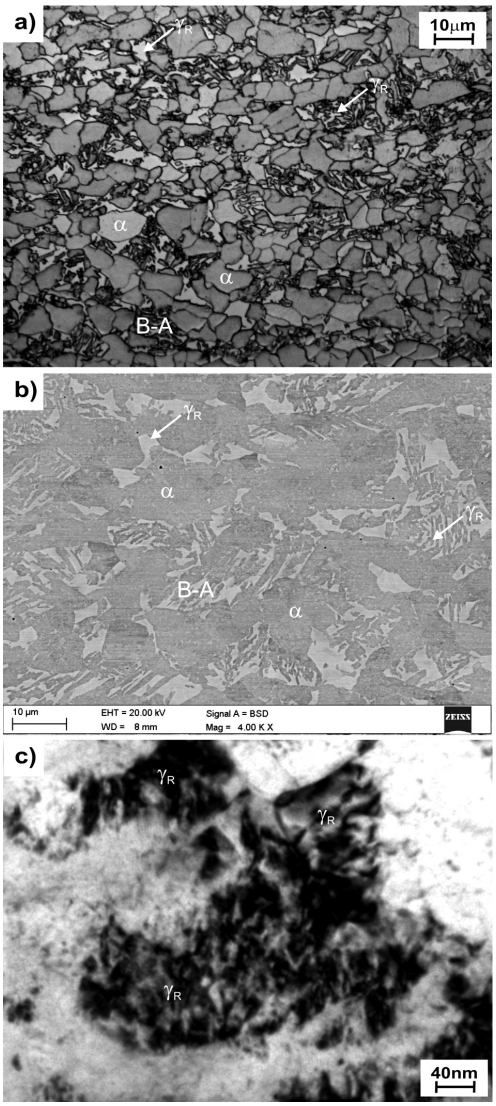

Figure 1: a), b) Fine-grained ferritic matrix containing bainitic-austenitic and austenitic islands after the thermomechanical processing and c) the finest regions of the retained austenite; α – ferrite, B-A – bainitic-austenitic islands, γ_R – retained austenite

Slika 1: a), b) Drobnozrnata feritna osnova vsebuje po termomehanski obdelavi bainitno-avstenitne in avstenitne otočke in c) najdrobnejša področja zaostalega avstenita; α – ferit, B-A – bainitnoavstenitni otočki, γ_R – zaostali avstenit

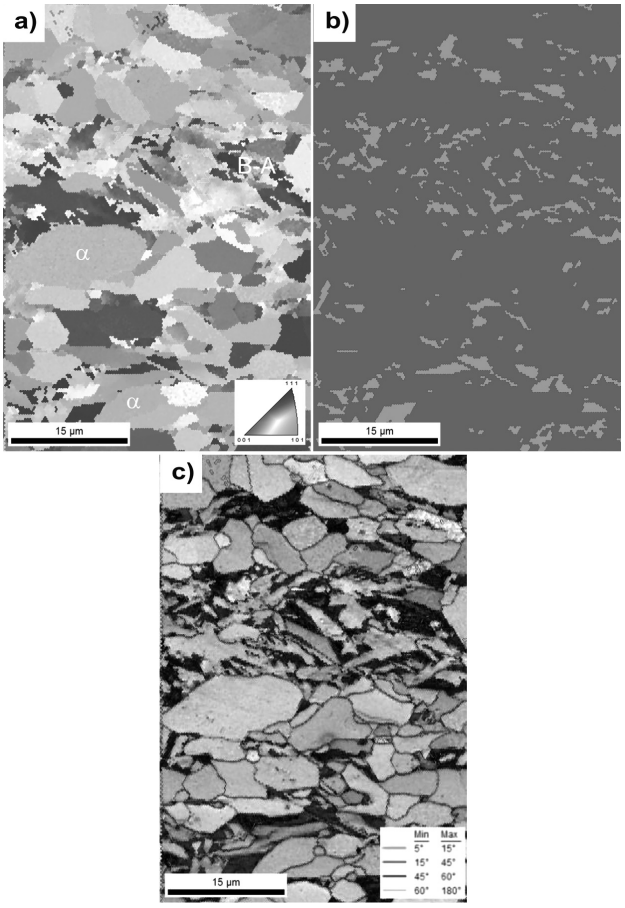

Figure 2: Microstructure images of the thermomechanically processed steel obtained with EBSD: a) inverse pole-figure map showing the grains with different crystallographic orientations, b) marked regions of the retained austenite, c) image-quality map with crystallographic misorientation angles

Slika 2: EBSD-posnetki mikrostrukture termomehansko predelanega jekla: a) zemljevid inverznih polovih figur, ki prikazuje zrna z različno kristalografsko orientacijo, b) označena področja zaostalega avstenita, c) zemljevid kvalitete zrn s kristalografsko različnimi koti

X-ray analysis equals mass fraction 1.14 %, which corresponds to lowering the martensite start temperature of the γ phase to about 10 °C. The mean ferrite grain size is equal to 6 μm and the retained austenite is located along the ferrite boundaries as blocky grains with the size up to 5 μm. Some retained austenite forms a halo around the α-phase grains whereas another part is located at the ferrite-bainite interfaces. A large fraction of the retained austenite, formed as thin layers or small blocky grains with the size of between 1 μm and 3 μm, is a constituent of the bainitic islands (B-A) (**Figure 1b**). A utilization of TEM reveals the finest regions of the retained austenite with the sizes from 50 nm to 200 nm (**Figure 1c**).

Figure 2 is an EBSD map using colour coding for determining individual grains. The inverse-pole figure (**Figure 2a**) shows the crystal direction parallel to the normal direction of the specimen using the colour coding according to the unit triangle. The grains of the highest size with a random crystallographic orientation can be recognized as ferrite. In the grey-scale image-quality (IQ) map (**Figure 2c**) they correspond to the brightest regions of the best diffraction quality. The IQ factor represents a quantitative description of the sharpness of the EBSD pattern. A lattice distorted by crystalline defects such as dislocations and subgrain boundaries has a distorted Kikuchi pattern, leading to lower IQ values.[7,8] The retained austenite, bainite and grain boundaries are represented by different levels of dark grey because their pattern contrast is lower than that of the ferrite. The color-coded phase map in **Figure 2b** clearly shows the distribution of the retained austenite. The BCC constituents and the retained austenite are distinguished on the basis of the differences in their crystal structures, whereas for a discrimination of the bainite from the ferrite the differences in the IQ values have to be used.

Due to a very small size of the retained austenite, its phase map is highly fragmented. The grain area of the retained-austenite particles covers a range of up to 14 μm^2 but the majority of the grains is smaller than 6 μm^2 (**Figure 3**). Having the knowledge of the retained-austenite presence and analyzing the IQ map in **Figure 2c** as well as the misorientation-angle distribution of the retained austenite (**Figure 4**), it is possible to indicate the bainite regions. Firstly, this phase always occurs in conjunction with the retained austenite and, secondly, having high-lattice imperfections, it corresponds to the dark regions of the low IQ. High-angle boundaries (> 15°) occur between the ferrite grains, BCC constituents and the retained austenite as well as between the ferrite and the bainite (**Figure 2c**). A large fraction of the retained austenite exhibits a misorientation angle close to 45° with the neighboring BCC constituents (**Figure 4**). This is in line with the earlier results obtained by Zaefferer et al.[19] for the 0.2C-1.4Mn-0.5Si-0.7Al steel and Petrov et al.[7], Wasilkowska et al.[18] for the 0.2C-1.5Mn-1.5Si steel, according to which bainite regions require a Kurdjumov-Sachs (K-S) or Nishiyama-Wasserman

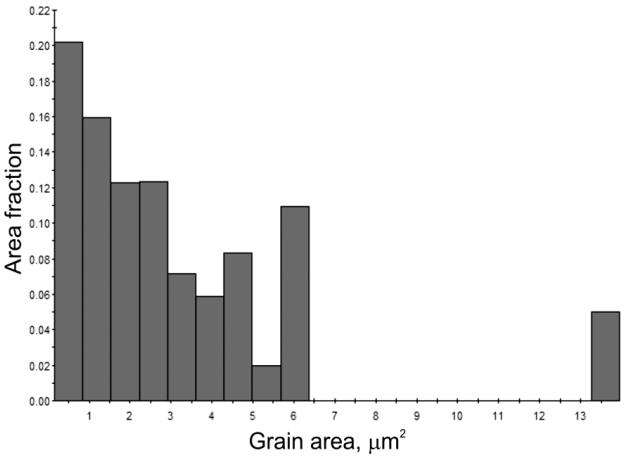

Figure 3: Distribution of the retained-austenite grain area

Slika 3: Razporeditev področij zrn zaostalega avstenita

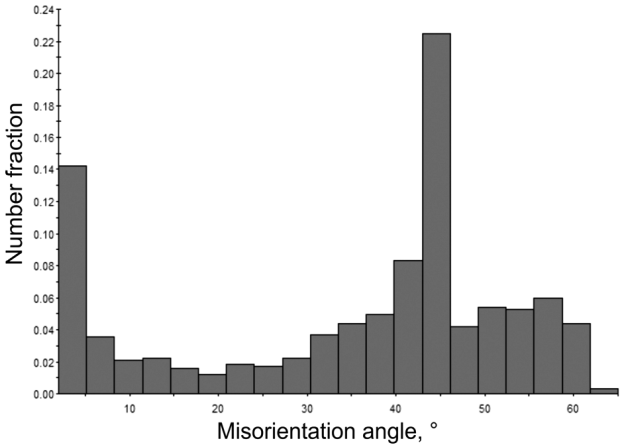

Figure 4: Distribution of the crystallographic misorientation angles of the grains

Slika 4: Razporeditev zrn z različnimi kristalografskimi koti

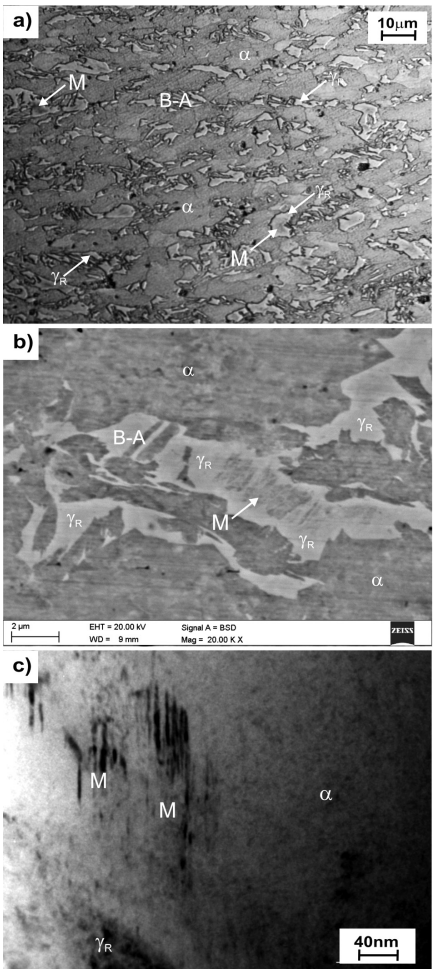

Figure 5: a), b) Ferritic-bainitic microstructures containing the retained austenite and strain-induced martensite of the steel strained to the elongation of 10 %, c) plate morphology of the strain-induced martensite; α – ferrite, B-A – bainitic-austenitic islands, γ_R – retained austenite, M – martensite

Slika 5: a), b) Feritno-bainitna mikrostruktura z zaostalim avstenitom in napetostno induciranim martenzitom v jeklu z 10-odstotno natezno deformacijo, c) ploščata morfologija napetostno induciranega martenzita; α – ferit, B-A – bainitno-avstenitni otočki, γ_R – zaostali avstenit, M – martenzit

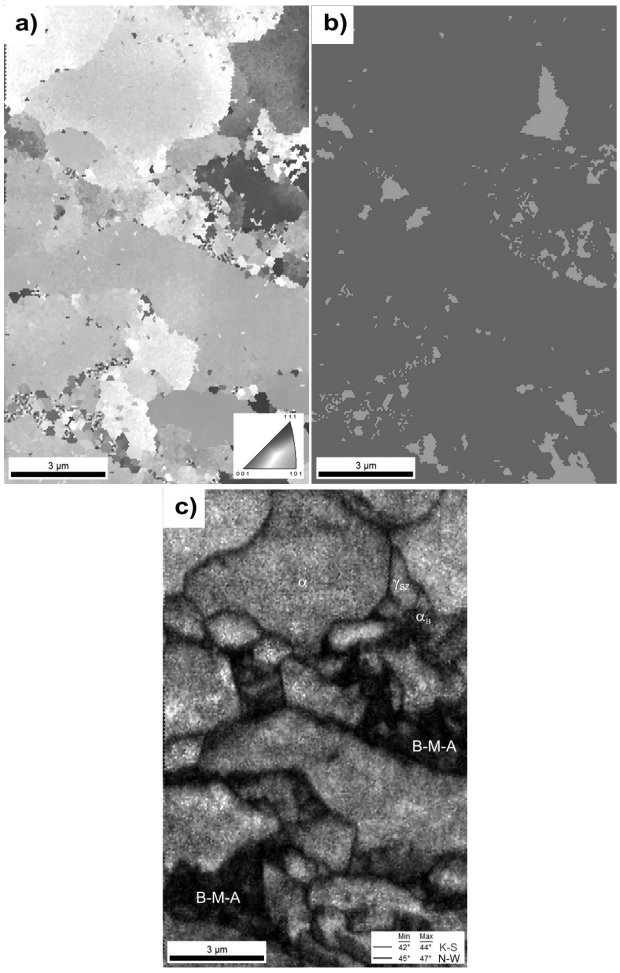

Figure 6: Microstructure images of the steel strained to the elongation of 10 %: a) inverse pole-figure map showing grains with different crystallographic orientations, b) marked regions of the retained austenite, c) image-quality map with the crystallographic misorientation angles corresponding to the K-S and N-W relationships; α – ferrite, α_B – bainitic ferrite, B-M-A – bainitic-martensitic-austenitic regions, γ_{SZ} – retained austenite

Slika 6: Posnetki mikrostrukture jekla, natezno obremenjenega do raztezka 10 %: a) zemljevid inverznih polovih figur, ki prikazujejo zrna z različno kristalografsko orientacijo, b) označena področja zaostalega avstenita, c) zemljevid kvalitete z različnimi kristalografskimi koti, ustrezno razmerjem K-S in N-W; α – ferit, α_B – bainitni ferit, B-M-A – bainitno-martenzitno-avstenitno področje, γ_{SZ} – zaostali avstenit

(N-W) orientation for their growth, confirming a displacive growth mechanism of bainite.

The γ-phase content decreases to about 7.7 % after applying a 10 % tensile strain. It corresponds to the 44 % initial austenite volume fraction transformed into martensite due to a strain-induced transformation. Generally, the strain-induced martensitic transformation initially proceeds in the largest and medium-sized austenite grains located in a ferritic matrix (**Figure 5a**). Martensite usually forms in the central zones of the grains whereas the borders remain untransformed (**Figure 5b**). This confirms a higher enrichment in carbon of the regions adjacent to the ferrite grains and a smaller enrichment of the central austenite regions as a result of a longer

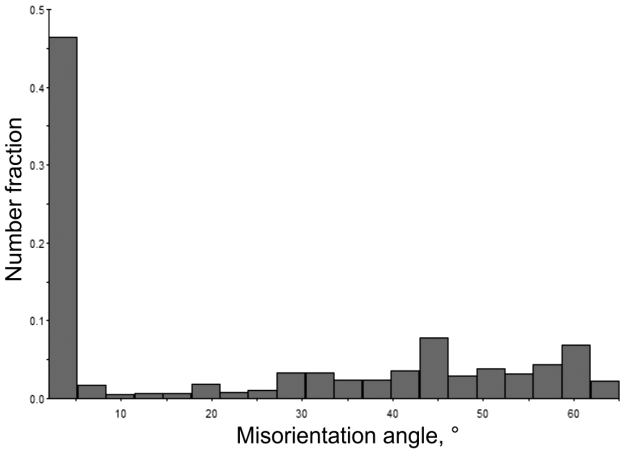

Figure 7: Distribution of crystallographic misorientation angles of the grains after cold deformation
Slika 7: Razporeditev zrn s kristalografsko različnimi koti po hladni deformaciji

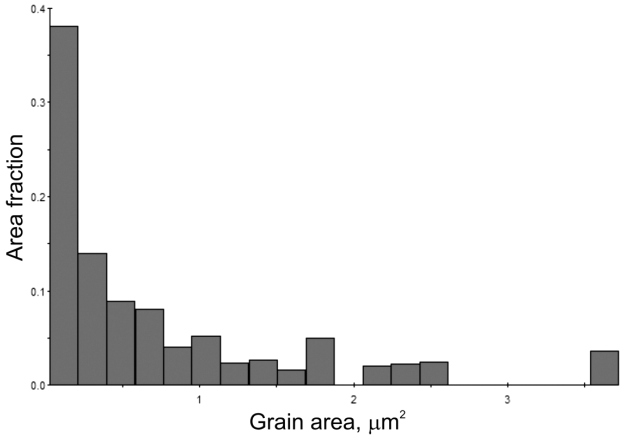

Figure 8: Distribution of the retained-austenite grain area of the cold-deformed steel
Slika 8: Razporeditev področij zrn zaostalega avstenita hladno deformiranega jekla

diffusion path of carbon. The formed martensite has a plate morphology (**Figure 5c**) and it contributes to a fragmentation of the untransformed austenite fostering its further stabilization due to a reduction in the particle size. It is clear from **Figure 6** that the strain-induced martensitic transformation is also initiated inside the largest bainitic-austenitic islands resulting in a further fragmentation of γ-phase particles. Moreover, the detailed analysis from **Figure 6c** indicates that the K-S and N-W relationships are partially kept between the austenite and the bainitic ferrite. However, the fraction fulfilling the special crystallographic orientations decreases (**Figure 7**) compared to the initial state (**Figure 4**). The fragmentation of the retained austenite is revealed through a reduction of the grain-size area below 4 μm^2 (**Figure 8**). It should be noted that the fraction of the grain area changes roughly in proportion to the inverse of the particle size.

4 CONCLUSIONS

A detailed identification of the morphological features of individual microstructural constituents of thermomechanically processed multiphase steels is a challenging problem due to a high dispersion of particular phases. The problem becomes even more complicated during cold deformation, when the highly dispersed retained austenite transforms into the strain-induced martensite. It was shown that the investigated Si-Al TRIP steel is characterized by a fine-grained ferritic matrix containing bainitic-austenitic and austenitic islands. The retained austenite occurs as small blocky grains or thin layers forming bainitic-austenitic islands. The strain-induced martensite initially forms in large and medium-sized austenite grains located along the boundaries of the α phase. The transformation is initiated in the central parts of the grains whereas the border regions of the austenite remain untransformed. The essential effect increasing the stability of the retained austenite against the strain-induced martensite is a fragmentation of the γ-phase regions. This effect is additionally enhanced by the neighboring bainitic-ferrite laths and the formed plate martensite creating a hydrostatic pressure against the deformation progress.

5 REFERENCES

[1] M. Pouranvari, E. Ranjbarnoodeh, Mater. Tehnol., 46 (**2012**) 6, 665–671
[2] M. Weglowski, K. Kwiecinski, K. Krasnowski, R. Jachym, Arch. Civ. Mech. Eng., 9 (**2009**), 85–97
[3] M. Pernach, K. Bzowski, R. Kuziak, M. Pietrzyk, Mater. Sci. Forum, 762 (**2013**), 699–704
[4] Z. Gronostajski, A. Niechajowicz, S. Polak, Arch. Metall. Mater., 55 (**2010**), 221–230
[5] S. Wiewiorowska, Steel Res. Int., 81 (**2010**), 262–265
[6] A. Kokosza, J. Pacyna, Arch. Metall. Mater., 55 (**2010**), 1001–1006
[7] R. Petrov, L. Kestens, A. Wasilkowska, Y. Houbaert, Mater. Sci. Eng. A, 447 **(2007)**, 285–297
[8] A. Grajcar, K. Radwanski, H. Krzton, Solid State Phenom., 203–204 (**2013**), 34–37
[9] I. B. Timokhina, P. D. Hodgson, E. V. Pereloma, Metall. Mater. Trans. A, 35 **(2004)**, 2331–2341
[10] J. Jung, S. J. Lee, S. Kim, B. C. De Cooman, Steel Res. Int., 82 (**2011**), 857–865
[11] D. A. Skobir, Mater. Tehnol., 45 (**2011**) 4, 295–301
[12] J. Majta, K. Muszka, Mater. Sci. Eng. A., 464 (**2007**), 186–191
[13] D. A. Skobir, M. Godec, M. Balcar, M. Jenko, Mater. Tehnol., 44 (**2010**) 6, 343–347
[14] A. Lisiecki, Proc. of the 10th Conf. on Laser Technology – Applications of Lasers, 8703 (**2013**), DOI: 10.1117/12.2013429
[15] M. Opiela, A. Grajcar, Arch. Civ. Mech. Eng., 12 (**2012**), 427–435
[16] C. P. Scott, J. Drillet, Scripta Mater., 56 (**2007**), 489–492
[17] J. Wu, P. J. Wray, C. I. Garcia, M. Hua, A. J. DeArdo, ISIJ Int., 45 (**2005**), 254–262
[18] A. Wasilkowska, R. Petrov, L. Kestens, E. A. Werner, C. Krempaszky, S. Traint, A. Pichler, ISIJ Int., 46 (**2006**), 302–309
[19] S. Zaefferer, J. Ohlert, W. Bleck, Acta Mater., 52 (**2004**), 2765–2778